International Journal of Signal Processing, Image Processing and Pattern Recognition
Vol.7, No.5 (2014), pp.1-12
http://dx.doi.org/10.14257/ijsip.2014.7.5.01

Image Edge Detection Based on Anti-Symmetrical Biorthogonal Wavelet Filter Banks with the Same Even Length

Xiaoyan Wang[1], Baochen Jiang[1,2], Chengyou Wang[1,*], Zhiqiang Yang[1,3] and Chunxiao Zhang[1]
[1] *School of Mechanical, Electrical and Information Engineering, Shandong University, Weihai 264209, P. R. China*
[2] *School of Electronic Information Engineering, Tianjin University, Tianjin 300072, P. R. China*
[3] *Integrated Electronic Systems Lab Co. Ltd., Jinan 250100, P. R. China*
swwxy00800313@163.com, jbc@sdu.edu.cn, wangchengyou@sdu.edu.cn, yangzhiqiang@ieslab.cn, sdwhzcx@126.com

Abstract

With the development of the theory of wavelet transform, biorthogonal wavelet filter banks with linear phase and compact support characteristics are widely used in signal and image processing. We study the multiscale edge detection using anti-symmetrical biorthogonal wavelet filter banks with the same even length based on the analysis of the properties of this wavelet filter banks. The steps of multiscale edge detection based on anti-symmetrical biorthogonal wavelet are introduced in detail. Experimental results on test images show that compared with the anti-symmetrical biorthogonal wavelet, the proposed anti-symmetrical biorthogonal wavelet filter banks with the same even length have better performance in terms of image edge detection. Therefore, the anti-symmetrical biorthogonal wavelet filter banks with the same even length are more suitable for image edge detection.

Keywords: *Image Processing, Multiscale Edge Detection, Filter Banks, Anti-symmetrical Biorthogonal Wavelet*

1. Introduction

Edge defines the boundaries between regions in an image, so edge detection is an important content of image processing. Due to excellent local time-frequency and multiresolution analysis characteristic, wavelet transform especially biorthogonal transform is widely used in signal and image processing, such as signal denoising [1], image compression [2], multiscale edge detection [3], singularity detection [4], image segmentation [5], *etc.*, Yang, *et al.*, proposed an improved method of image edge detection based on wavelet transform [6]. Zhang, *et al.*, proposed a novel edge detection method based on the fusion of wavelet transform and mathematical morphology [7].

On the basis of analyzing Mallat algorithm [8], Hou, *et al.*, [9] presented two kinds of boundary extension methods, point-symmetric extension (PSE) and edge-symmetric extension (ESE) commonly used in finite length signal processing. They preserve the perfect reconstruction while keeping the signal length unchanged.

In the past decades, the construction of biorthogonal wavelet had been studied and many kinds of wavelets were constructed [10-12]. Liu, *et al.*, [13] constructed a new kind of biorthogonal wavelet filter banks, named anti-symmetrical biorthogonal wavelet filter banks with the same even length. Design formulas and steps were described in detail. Particularly,

ISSN: 2005-4254 IJSIP

the properties of this wavelet filter banks were studied and the differential operator property was analyzed. In this paper, we explore its application in image edge detection, and compare it with other anti-symmetrical biorthogonal wavelet [14].

The rest of this paper is organized as follows. In Section 2, the anti-symmetrical biorthogonal wavelet filter banks with the same even length and the differential operator property are presented. Section 3 introduces the Mallat algorithm for finite length signal. In Section 4, the process of multiscale edge detection based on anti-symmetrical biorthogonal wavelet is introduced in detail. Experimental results of multiscale edge detection using anti-symmetrical biorthogonal wavelet and anti-symmetrical biorthogonal wavelet filter banks with the same even length are presented in Section 5. Finally, conclusions are given in Section 6.

2. Anti-symmetrical Biorthogonal Wavelet Filter Banks with the Same Even Length

2.1. Differential Operator Property

Supposed the support interval of sequence $\{q_k\}$ is $\mathrm{supp}\{q_k\} = [-K+1, K]$, $K > 0$, i.e.

$$\{q_k\} = \{q_{-K+1}, \cdots, q_{-1}, q_0, q_1, \cdots, q_{K-1}, q_K\}, \tag{1}$$

and

$$q_k = -q_{1-k}, \ k = 1, 2, \cdots, K. \tag{2}$$

We define a new sequence $\{c_k\}$

$$c_k = \sqrt{2} \sum_{j=k+1}^{K} q_j, \ k \in [-K, K-1]. \tag{3}$$

Because of $\sum_{k=-K+1}^{K} q_k = 0$, we get

$$c_{-K} = \sqrt{2} \sum_{j=K+1}^{K} q_j = 0. \tag{4}$$

Therefore, the support interval of sequence $\{c_k\}$ is $[-(K-1), K-1]$ with length of $2K-1$. And as a result of

$$\sum_{j=-(k-1)}^{k} q_j = 0, \ \forall k \in [-(K-1), K], \tag{5}$$

we have

$$c_{-k} = \sqrt{2} \sum_{j=-k+1}^{K} q_j = \sqrt{2} \sum_{j=-k+1}^{K} q_j + \sqrt{2} \sum_{j=-k}^{k+1} q_j = \sqrt{2} \sum_{j=k+1}^{K} q_j = c_k. \tag{6}$$

So the sequence $\{c_k\}$ is even symmetrical about $k = 0$ [13].

According to Eq. (3), the definition of sequence $\{c_k\}$, we know $\sqrt{2} q_k = c_{k-1} - c_k$. Using the two-scale relation

$$\tilde{\psi}(t) = \sqrt{2} \sum_{k=-\infty}^{\infty} \tilde{q}_k \tilde{\varphi}(2t-k), \ \psi(t) = \sqrt{2} \sum_{k=-\infty}^{\infty} q_k \varphi(2t-k), \tag{7}$$

we have

$$\begin{aligned}\psi(t) &= \sqrt{2}\sum_{k=-(K-1)}^{K} q_k \varphi(2t-k) = \sum_{k=-(K-1)}^{K} (c_{k-1} - c_k)\varphi(2t-k) \\ &= \sum_{k=-(K-2)}^{K} c_{k-1}\varphi(2t-k) - \sum_{k=-(K-1)}^{K-1} c_k \varphi(2t-k) \\ &= \sum_{k=-(K-1)}^{K-1} c_k \varphi(2t-k-1) - \sum_{k=-(K-1)}^{K-1} c_k \varphi(2t-k).\end{aligned} \tag{8}$$

Because that the value of $|q_k|$ decreases with the increase of $|k|$ and that negative and positive values of sequence $\{c_k\}$ just cancel each other out in the sum of Eq. (3), the absolute value of central element c_0 in sequence $\{c_k\}$ is obviously greater than absolute value of others. Therefore, we can keep only the central part of Eq. (8), thus $\psi(t)$ can be approximately expressed as

$$\psi(t) \approx c_0 \left(\varphi(2t-1) - \varphi(2t)\right). \tag{9}$$

If $\varphi(t)$ is smooth enough, as for Eq. (9), in virtue of Lagrange mean value theorem, it becomes

$$\psi(t) \approx c_0 \frac{\mathrm{d}}{\mathrm{d}t}\varphi(2t-0.5). \tag{10}$$

This means that $\psi(t)$ possesses the property of differential operator. According to duality, we know that $\tilde{\psi}(t)$ has the property of differential operator too. The functions $\tilde{\psi}(t)$ and $\psi(t)$ are suitable for image edge detection.

2.2. Other Properties

(a) $\{\tilde{p}_k\}$, $\{p_k\}$, $\{\tilde{q}_k\}$ and $\{q_k\}$ have the same support interval $\mathrm{supp} = [-K+1, K]$, $K > 0$;

(b) $\{\tilde{p}_k\}$ and $\{p_k\}$ are symmetric about 0.5, i.e. $\tilde{p}_k = \tilde{p}_{1-k}$, $p_k = p_{1-k}$, $k = 1, 2, \cdots, K$;

(c) $\{\tilde{q}_k\}$ and $\{q_k\}$ are anti-symmetric about 0.5, i.e. $\tilde{q}_k = -\tilde{q}_{1-k}$, $q_k = -q_{1-k}$, $k = 1, 2, \cdots, K$;

(d) $\tilde{\varphi}(t)$, $\varphi(t)$, $\tilde{\psi}(t)$ and $\psi(t)$ have the same support interval $\mathrm{supp} = [-K+1, K]$, $K > 0$, $\tilde{\varphi}(t)$ and $\varphi(t)$ are symmetric about 0.5, while $\tilde{\psi}(t)$ and $\psi(t)$ are anti-symmetric about 0.5.

3. Mallat Algorithm for Finite Length Signal

In the derived process of Mallat algorithm, the length of input sequence $\{c_{j,k}\}$ is assumed to be infinite. The decomposition algorithm is

$$\begin{cases} c_{j-1,k} = \sum_{l\in\mathbf{Z}} \tilde{p}_{l-2k} c_{j,l} = \sum_{l\in\mathbf{Z}} \tilde{p}_{l-k'} c_{j,l}\Big|_{k'=2k}, \\ d_{j-1,k} = \sum_{l\in\mathbf{Z}} \tilde{q}_{l-2k} c_{j,l} = \sum_{l\in\mathbf{Z}} \tilde{q}_{l-k'} c_{j,l}\Big|_{k'=2k}. \end{cases} \tag{11}$$

The reconstruction algorithm is

$$\begin{aligned} c_{j,k} &= \sum_{l\in \boldsymbol{Z}} \left[p_{k-2l} c_{j-1,l} + q_{k-2l} d_{j-1,l} \right] \\ &= \sum_{l\in \boldsymbol{Z}} \left[p_{k-2l} c_{j-1,l} + q_{k-2l} d_{j-1,l} \right] + \sum_{l\in \boldsymbol{Z}} \left[p_{k-2l+1} \cdot 0 + q_{k-2l+1} \cdot 0 \right] \\ &= \sum_{l\in \boldsymbol{Z}} \left[p_{k-l} c'_{j-1,l} + q_{k-l} d'_{j-1,l} \right], \end{aligned} \tag{12}$$

where $\{c'_{j-1,l}\}, \{d'_{j-1,l}\}$ are obtained from $\{c_{j-1,l}\}, \{d_{j-1,l}\}$ by adding zero in odd index. In Eqs. (11) and (12), $\{c_{j-1,k}\}$ and $\{d_{j-1,k}\}$ are infinite sequences, where $k \in \boldsymbol{Z}$. However, we can only acquire the finite sample of continuous function $f(t),\ t \in \boldsymbol{R}$ or discrete sequence $\{f_k\},\ k \in \boldsymbol{Z}$ in applications [9].

The flow chart of Mallat algorithm for finite length sequence is shown in Figure 1. The decomposition algorithm in Eq. (11) can be rewritten as

$$c'_{N-1,k} = \sum_{l=-N_1}^{N_2} \tilde{p}_l c_{N,k+l},\ d'_{N-1,k} = \sum_{l=-N'_1}^{N'_2} \tilde{q}_l c_{N,k+l}, \tag{13}$$

$$c_{N-1,k} = c'_{N-1,2k},\ d_{N-1,k} = d'_{N-1,2k}. \tag{14}$$

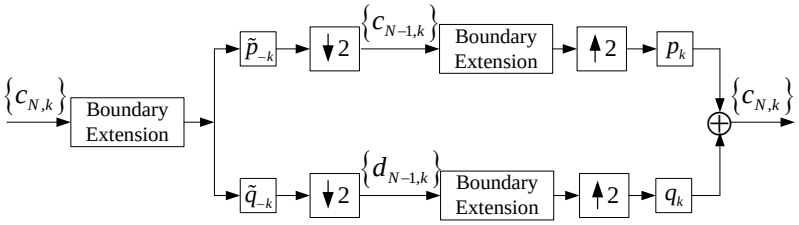

Figure 1. Mallat Algorithm of Finite Length Sequence

Taking anti-symmetrical biorthogonal wavelet filter banks with the same even length Bior3.1 as an example, coefficients of these filter banks are as follows:

$$\{\tilde{p}_k\} = \{\tilde{p}_{-1} \sim \tilde{p}_2\} = \{0.1768,\ 0.5303,\ 0.5303,\ 0.1768\};$$

$$\{\tilde{q}_k\} = \{\tilde{q}_{-1} \sim \tilde{q}_2\} = \{0.3536,\ 1.0607,\ -1.0607,\ -0.3536\};$$

$$\{p_k\} = \{p_{-1} \sim p_2\} = \{-0.3536,\ 1.0607,\ 1.0607,\ -0.3536\};$$

$$\{q_k\} = \{q_{-1} \sim q_2\} = \{-0.1768,\ 0.5303,\ -0.5303,\ 0.1768\}.$$

The decomposition and reconstruction flow charts of $\{c_{N,k}\} = \{162,\ 163,\ 166,\ 162,\ 155,\ 160,\ 157,\ 161\}$ ($L = 8$) obtained from image Lena are shown in Figure 2.

4. Multiscale Edge Detection Algorithm

The wavelet transform of image at each scale provides much edge information. Multiscale edge detection realizes the combination of edge information at each scale in order to get ideal edge. The algorithm of multiscale edge detection is introduced in detail as follows.

(1) Anti-symmetrical biorthogonal wavelet is applied to wavelet decomposition process, four areas are derived: horizontal and vertical low frequency information (LL) called

approximate component; horizontal high frequency and vertical low frequency information (HL); horizontal low frequency and vertical high frequency information (LH); horizontal and vertical high frequency information (HH) [15]. Then the same decomposition process is performed on horizontal and vertical low frequency information.

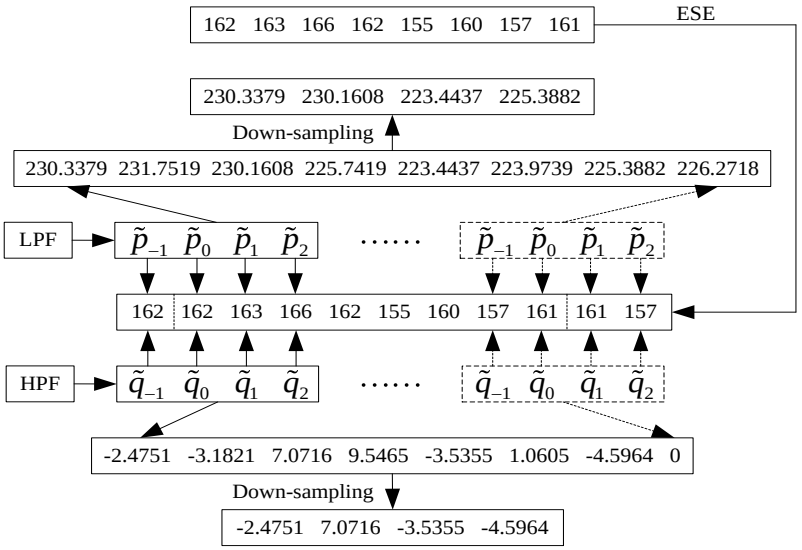

(a)

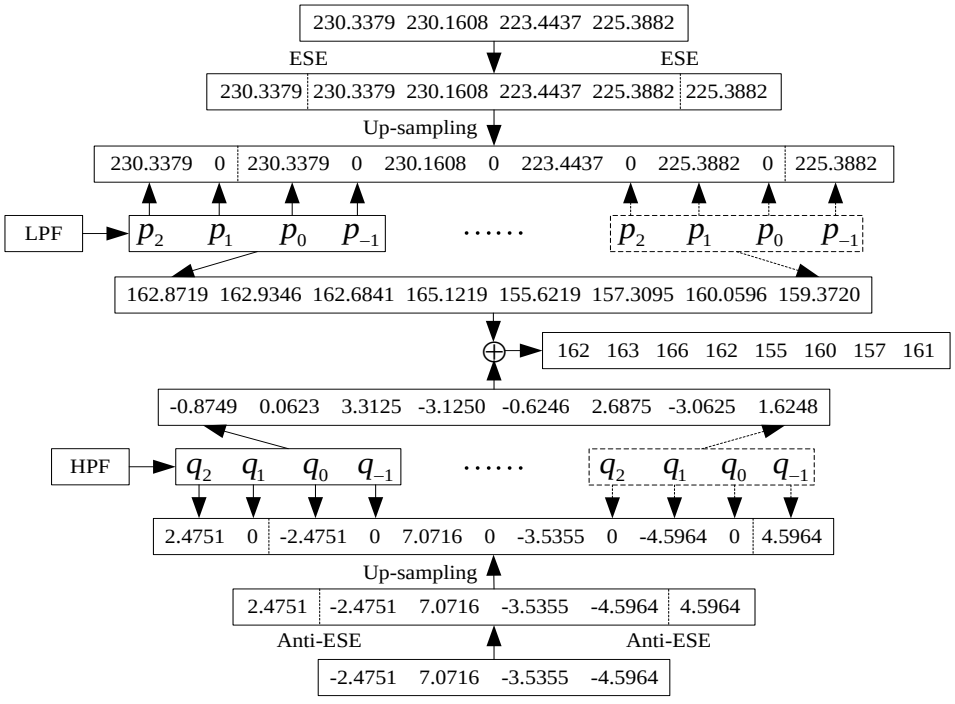

(b)

Figure 2. An Example of ESE with Image Data ($L = 8$): (a) The Decomposition Process, (b) The Reconstruction Process

(2) Based on the pyramidal decomposition data of image, we compute modulus image $M_{2^j} f(x,y)$ and angle image $A_{2^j} f(x,y)$ at each scale 2^j, $j = -1,-2,\cdots,-J$. The modulus of the gradient vector is obtained by

$$M_{2^j} f(x,y) = \sqrt{\left|W^1_{2^j} f(x,y)\right|^2 + \left|W^2_{2^j} f(x,y)\right|^2}. \quad (15)$$

The angle of the gradient vector is computed by

$$A_{2^j} f(x,y) = \arctan\left(\frac{W^1_{2^j} f(x,y)}{W^2_{2^j} f(x,y)}\right), \quad (16)$$

where $W^1_{2^j} f(x,y)$ is the horizontal high frequency and vertical low frequency information at each scale 2^j, and $W^2_{2^j} f(x,y)$ means the horizontal low frequency and vertical high frequency information at each scale 2^j.

(3) For each scale 2^j, we detect the local maxima of $M_{2^j} f(x,y)$ along the direction given by angle image $A_{2^j} f(x,y)$ [16]. There are four possible directions for gradient vector, respectively, 0°, 90°, 45° and 135°. For any point (m,n) of $M_{2^j} f(x,y)$, if the modulus of it is the local maxima of the ones of three points on the direction of gradient vector, we record (m,n) as candidate edge point. All candidate edge points constitute edge image $B_{2^j} f(x,y)$.

(a) If the direction of gradient vector is 0°, we compare the following three points: $(m-1,n)$, (m,n) and $(m+1,n)$.

(b) If the direction of gradient vector is 90°, we compare the following three points: $(m,n-1)$, (m,n) and $(m,n+1)$.

(c) If the direction of gradient vector is 45°, we compare the following three points: $(m-1,n-1)$, (m,n) and $(m+1,n+1)$.

(d) If the direction of gradient vector is 135°, we compare the following three points: $(m+1,n-1)$, (m,n) and $(m-1,n+1)$.

(4) Due to the presence of noise and fine texture, there are many pseudo-edge points in the set of edge points. Based on the property of smaller modulus of pseudo-edge point, we can adopt the threshold method to eliminate those points whose moduluses are smaller than the specified threshold from edge image.

(5) We synthesize the obtained edge information in order to get the precise and single pixel wide edge according to the set of edge points at each scale 2^j. The process of multiscale combination is introduced in detail as follows.

Step 1. At the scale $2^j, j = -J$, we link those points with similar moduli and angles from the thresholded edge image $B_{2^j} f(x,y)$. Then the length and average modulus of each chain are computed. For each chain, if the length of it is shorter than the specified chain length threshold L_{2^j} or the average modulus is smaller than the specified link modulus threshold T_{2^j}, we remove it. Therefore the single pixel wide edge image $E_{2^j} f(x,y), j = -J$ is obtained.

Step 2. For each edge point in $E_{2^j} f(x,y)$, we search the corresponding area in modulus maxima image $B_{2^{j+1}} f(x,y)$ with size of 3×3 to find all possible edge points.

These edge points constitute edge image. Those points with similar moduli and angles in obtained edge image are linked. The length and average modulus of each chain are analyzed. For each chain, if the length of it is shorter than the specified chain length threshold $L_{2^{j+1}}$ or the average modulus is smaller than the specified chain modulus threshold $T_{2^{j+1}}$, we remove it. In this way, we get the single pixel wide edge image $E_{2^{j+1}} f(x, y)$.

Step 3. The Step 2 is repeated until $j = -1$.

5. Experimental Results

Any anti-symmetrical biorthogonal wavelet which meets the conditions of the differential operator can be used to image edge detection. Simulation experiments are conducted using MATLAB 7.8. To test the edge detection performance of the anti-symmetrical biorthogonal wavelet filter banks with the same even length, Lena (8bits/pixel, 512×512) is used in simulation experiments as test image. In the following, anti-symmetrical biorthogonal wavelet filter banks with the same even length Bior3.1, Bior5.1 and Bior7.1 are tested, and compared with anti-symmetrical biorthogonal wavelet Bior1.3 which has best performance in edge detection [14]. In multiscale edge detection algorithm, we set wavelet decomposition parameter $J = 3$.

The coefficients of Bior5.1 are shown as follows:

$$\{\tilde{p}_k\} = \{\tilde{p}_{-2} \sim \tilde{p}_3\} = \{0.0442,\ 0.2210,\ 0.4419,\ 0.4419,\ 0.2210,\ 0.0442\};$$

$$\{\tilde{q}_k\} = \{\tilde{q}_{-2} \sim \tilde{q}_3\} = \{0.2652,\ 1.3258,\ 1.7678,\ -1.7678,\ -1.3258,\ -0.2652\};$$

$$\{p_k\} = \{p_{-2} \sim p_3\} = \{0.2652,\ -1.3258,\ 1.7678,\ 1.7678,\ -1.3258,\ 0.2652\};$$

$$\{q_k\} = \{q_{-2} \sim q_3\} = \{0.0442,\ -0.2210,\ 0.4419,\ -0.4419,\ 0.2210,\ -0.0442\}.$$

The coefficients of Bior7.1 are shown as follows:

$$\{\tilde{p}_k\} = \{\tilde{p}_{-3} \sim \tilde{p}_4\} = \begin{Bmatrix} 0.0110, & 0.0773, & 0.2320, & 0.3867 \\ 0.3867, & 0.2320, & 0.0773, & 0.0110 \end{Bmatrix};$$

$$\{\tilde{q}_k\} = \{\tilde{q}_{-3} \sim \tilde{q}_4\} = \begin{Bmatrix} 0.2210, & 1.5468, & 4.0217, & 3.4030 \\ -3.4030, & -4.0217, & -1.5468, & -0.2210 \end{Bmatrix};$$

$$\{p_k\} = \{p_{-3} \sim p_4\} = \begin{Bmatrix} -0.2210, & 1.5468, & -4.0217, & 3.4030 \\ 3.4030, & -4.0217, & 1.5468, & -0.2210 \end{Bmatrix};$$

$$\{q_k\} = \{q_{-3} \sim q_4\} = \begin{Bmatrix} -0.0110, & 0.0773, & -0.2320, & 0.3867 \\ -0.3867, & 0.2320, & -0.0773, & 0.0110 \end{Bmatrix}.$$

The coefficients of Bior1.3 are shown as follows:

$$\{\tilde{p}_k\} = \{\tilde{p}_{-2} \sim \tilde{p}_3\} = \{-0.0884,\ 0.0884,\ 0.7071,\ 0.7071,\ 0.0884,\ -0.0884\};$$

$$\{\tilde{q}_k\} = \{\tilde{q}_0 \sim \tilde{q}_1\} = \{-0.7071,\ 0.7071\};$$

$$\{p_k\} = \{p_0 \sim p_1\} = \{0.7071,\ 0.7071\};$$

$$\{q_k\} = \{q_{-2} \sim q_3\} = \{-0.0884,\ -0.0884,\ 0.7071,\ -0.7071,\ 0.0884,\ 0.0884\}.$$

The multiscale edge detection results of the Lena image using Bior1.3, Bior3.1, Bior5.1 and Bior7.1 are shown in Figure 3. From the experimental results, we can see that compared with Bior1.3, the multiscale edge detection performances of Bior3.1,

Bior5.1 and Bior7.1 are all better in terms of the continuity of edge and edge positioning accuracy.

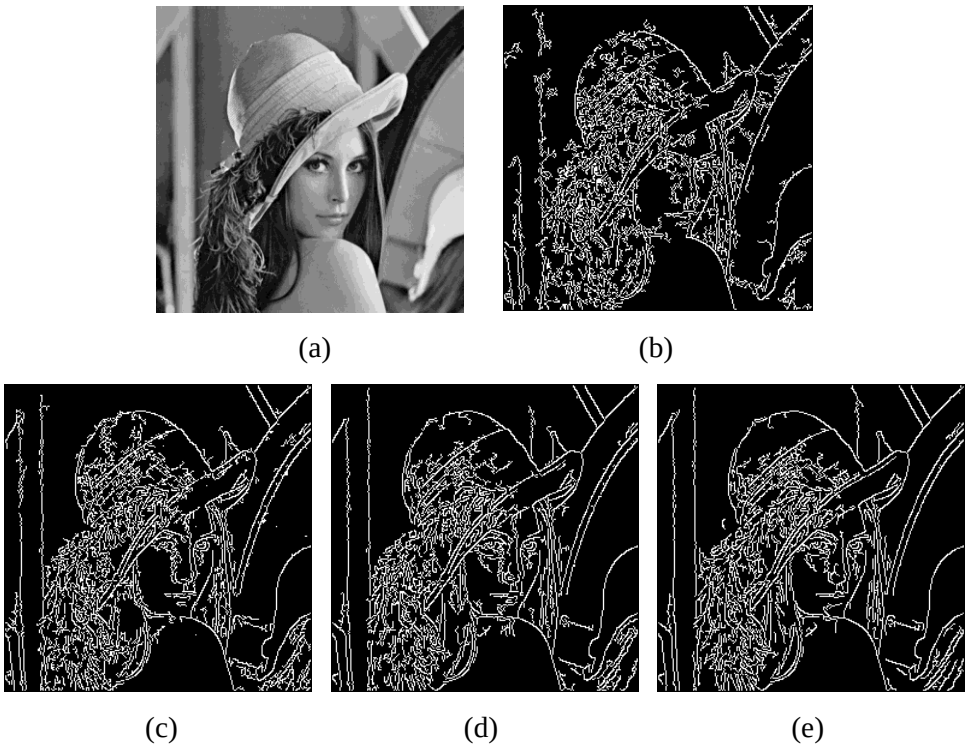

Figure 3. Edge Detection Results of Lena with Different Wavelets: (a) Lena, (b) Bior1.3, (c) Bior3.1, (d) Bior5.1, (e) Bior7.1

Figure 4(a) shows the image Lena with Gaussian noise whose mean value is 20 and variance is 36. While Bior1.3, Bior3.1, Bior5.1 and Bior7.1 applying on multiscale edge detection of noised Lena, the corresponding experimental results are shown in Figure 4(b)~(e). Apparently the multiscale edge detection results of noised Lena using Bior3.1, Bior5.1 and Bior7.1 are good, but the one using Bior1.3 is bad. Therefore the edge detection based on anti-symmetrical biorthogonal wavelet filter banks with the same even length has good anti-noise performance especially Bior5.1 and Bior7.1.

6. Conclusion

In this paper, anti-symmetrical biorthogonal wavelet filter banks with the same even length are introduced. Based on the analysis of properties of anti-symmetrical biorthogonal wavelet filter banks with the same even length, the multiscale edge detection algorithm using this wavelet filter banks is achieved. The experiments to typical test images are done in MATLAB. Compared with anti-symmetrical biorthogonal wavelet, the proposed algorithm using anti-symmetrical biorthogonal wavelet filter banks with the same even length has better performance in terms of edge detection. And the multiscale edge detection algorithm based on anti-symmetrical biorthogonal wavelet filter banks with the same even length shows good anti-noise performance.

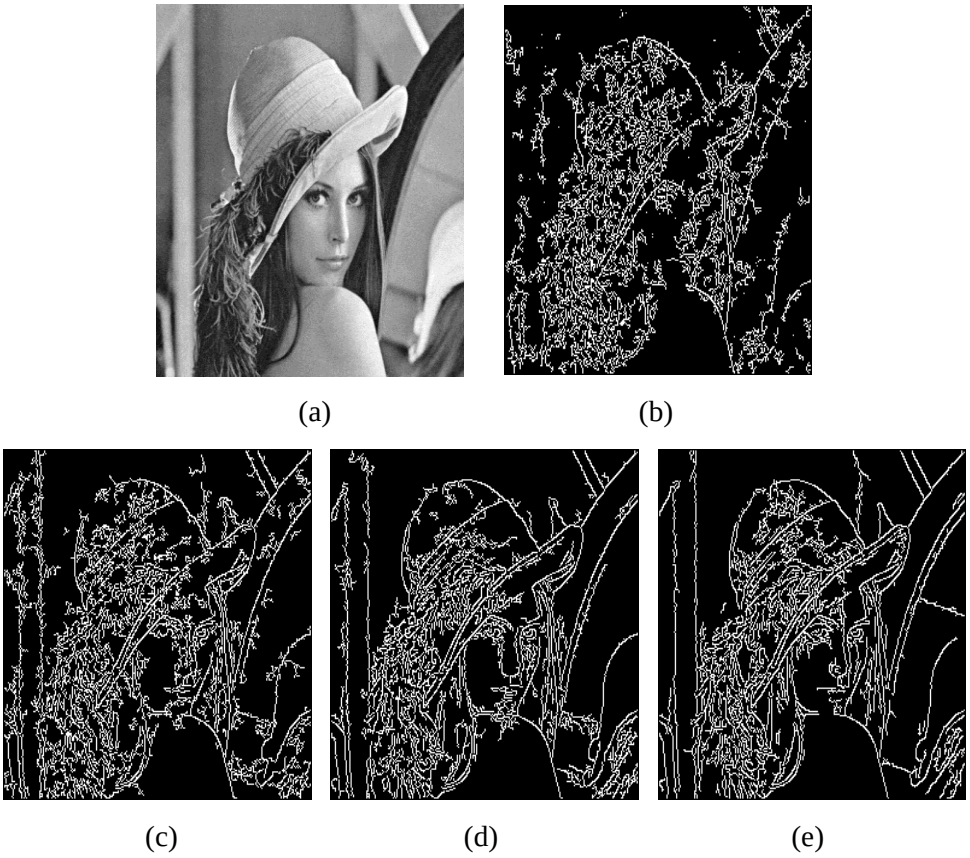

Figure 4. Edge Detection Results of Noised Lena with Different Wavelets: (a) Noised Lena, (b) Bior1.3, (c) Bior3.1, (d) Bior5.1, (e) Bior7.1

Acknowledgements

This work was supported by the Graduate Innovation Foundation of Shandong University at WeiHai (GIFSDUWH) (Grant No. yjs12028), the National Natural Science Foundation of China (Grant No. 61201371) and the promotive research fund for excellent young and middle-aged scientists of Shandong Province, China (Grant No. BS2013DX022). The authors would like to thank Fanfan Yang for her help and valuable suggestions. The authors also thank the anonymous reviewers and the editor for their valuable comments to improve the presentation of the paper.

References

[1] D. L. Donoho, "De-noising by soft-thresholding", IEEE Transactions on Information Theory, vol. 41, no. 3, (**1995**), pp. 613-627.
[2] D. Taubman, "High performance scalable image compression with EBCOT", IEEE Transactions on Image Processing, vol. 9, no. 7, (**2000**), pp. 1158-1170.
[3] T. Aydin, Y. Yemez, E. Anarim and B. Sankur, "Multidirectional and multiscale edge detection via M-band wavelet transform", IEEE Transactions on Image Processing, vol. 5, no. 9, (**1996**), pp. 1370-1377.
[4] S. Mallat and W. L. Hwang, "Singularity detection and processing with wavelets", IEEE Transactions on Information Theory, vol. 38, no. 2, (**1992**), pp. 617-643.

[5] B. G. Kim, J. I. Shim and D. J. Park, "Fast image segmentation based on multi-resolution analysis and wavelets", Pattern Recognition Letters, vol. 24, no. 16, (**2003**), pp. 2995-3006.
[6] H. Yang, C. S. Li, and L. Pei, "An improved method of image edge detection based on wavelet transform", Proceedings of the IEEE International Conference on Computer Science and Automation Engineering, Shanghai, China, (**2011**) June 10-12, pp. 678-681.
[7] W. J. Zhang and J. Y. Kang, "Edge detection based on fusion of wavelet transform and mathematical morphology", Proceedings of the International Conference on Information Engineering and Computer Science, Wuhan, China, (**2009**) December 19-20, pp. 1-4.
[8] S. Mallat, "Theory for multiresolution signal decomposition: the wavelet representation", IEEE Transactions on Pattern Analysis and Machine Intelligence, vol. 11, no. 7, (**1989**), pp. 674-693.
[9] Z. X. Hou, C. Y. Wang and A. P. Yang, "Study on symmetric extension methods in Mallat algorithm of finite length signal", Proceedings of the 5th International Conference on Visual Information Engineering, Xi'an, China, (**2008**) July 29- August 1, pp. 341-346.
[10] A. Cohen, I. Daubechies and J. C. Feauveau, "Biorthogonal bases of compactly supported wavelets", Communications on Pure and Applied mathematics, vol. 45, no. 5, (**1992**), pp. 485-560.
[11] C. K. Chui, "An Introduction to Wavelets", Academic Press, San Diego, CA, USA, (**1992**).
[12] L. H. Cui, Z. S. Pan and Z. X. Cheng, "Perfect reconstruction biorthogonal multi filter banks", Proceedings of the International Conference on Machine Learning and Cybernetics, Xi'an, China, vol. 5, (**2003**) November 2-5, pp. 2614-2619.
[13] J. Z. Liu, Z. X. Hou and C. Y. Wang, "Design and properties of anti-symmetrical biorthogonal wavelet filter banks with the same even length", Proceedings of the International Conference on Wavelet Analysis and Pattern Recognition, Baoding, China, (**2009**) July 12-15, pp. 319-323.
[14] G. R. Mo, J. Y. Peng, S. Q. Mo and M. H. Xie, "Fast signal reconstruction from modulus maxima based on anti-symmetrical biorthogonal wavelets", Journal of Electronics and Information Technology, vol. 29, no. 8, (**2007**) pp. 1860-1863.
[15] Q. Yin, Z. Y. Yuan, Y. Kong and P. Guo, "Face recognition research based on anti-symmetrical wavelet and eigenface", Proceedings of the 6th International Conference on Machine Learning and Cybernetics, Hong Kong, China, vol. 1, (**2007**) August 19-22, pp. 366-371.
[16] S. Mallat and S. Zhong, "Characterization of signals from multiscale edges", IEEE Transactions on Pattern Analysis and Machine Intelligence, vol. 14, no. 7, (**1992**), pp. 710-732.

Authors

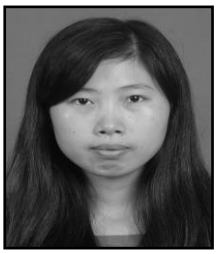

Xiaoyan Wang, she was born in Shandong province, China in 1990. She received her B.S. degree in electronic information science and technology from Shandong University, Weihai, China, in 2012. Now she is pursuing her M.E. degree in circuits and systems in Shandong University, Weihai, China. Her research interests concentrate on image and video processing.

Baochen Jiang, he was born in Shandong province, China in 1962. He received his B.S. degree in radio electronics from Shandong University, China, in 1983 and his M.E. degree in communication and electronic systems from Tsinghua University, China, in 1990. Now he is a professor in the School of Mechanical, Electrical and Information Engineering, Shandong University, Weihai, China. His current research interests include signal and information processing, image and video processing, and smart grid technology.

Chengyou Wang, he was born in Shandong province, China in 1979. He received his B.E. degree in electronic information science and technology from Yantai University, China, in 2004 and his M.E. and Ph.D. degree in signal and information processing from Tianjin University, China, in 2007 and 2010 respectively. Now he is an associate professor in the School of Mechanical, Electrical and Information Engineering, Shandong University, Weihai, China. His current research interests include digital image and video processing, wavelet analysis and its applications, multidimensional signal and information processing, and smart grid technology.

Zhiqiang Yang, he was born in Shandong province, China in 1954. He received his B.S. degree and M.E. degree in electronics from Shandong University, China. Now he is an associate professor in the School of Mechanical, Electrical and Information Engineering, Shandong University, Weihai, China and he is also with the Integrated Electronic Systems Lab Co. Ltd., Jinan, China. His current research interests include electronic information system, software and power system automation.

Chunxiao Zhang, he was born in Shandong province, China in 1990. He received his B.S. degree in electronic information science and technology from Shandong University, Weihai, China, in 2012. Now he is pursuing his M.E. degree in circuits and systems in Shandong University, Weihai, China. His research interests concentrate on image and video processing.

